Effective index of refraction, optical rotation, and circular dichroism in isotropic chiral liquid crystals

D. Lacoste,[1] P. J. Collings,[2] and T. C. Lubensky[1]
[1] *Department of Physics, University of Pennsylvania, Philadelphia, Pennsylvania 19104*
[2] *Department of Physics and Astronomy, Swarthmore College, Swarthmore, Pennsylvania 19081*
(Received 15 October 2001; published 5 March 2002)

This paper concerns optical properties of the isotropic phase above the isotropic-cholesteric transition and of the blue phase BP III. We introduce an effective index, which describes spatial dispersion effects such as optical rotation, circular dichroism, and the modification of the average index due to the fluctuations. We derive the wavelength dependence of these spatial dispersion effects quite generally without relying on an expansion in powers of the chirality and without assuming that the pitch of the cholesteric P is much shorter than the wavelength of the light λ, an approximation that has been made in previous studies of this problem. The theoretical predictions are supported by comparing them with experimental spectra of the optical activity in the BP III phase.

DOI: 10.1103/PhysRevE.65.031717 PACS number(s): 61.30.Mp, 42.70.Df, 78.20.Ek

I. INTRODUCTION

Chirality in liquid crystals produces a fascinating variety of phases, such as the blue phases. Three blue phases (BPs) designated BP I, BP II, and BP III have been identified and their structures are now well understood. BP I and BP II exhibit long-range periodic order at the half micron scale and Bragg scatter visible light. For these reasons, the optical study of blue phases is an active field of research, with a particular emphasis on spatial dispersion effects such as the optical activity.

The first experiments on the optical activity in the pretransitional region of the isotropic phase above the isotropic-cholesteric transition were carried out by Cheng and Meyer [1]. Using a general formulation due to de Gennes, they calculated and confirmed experimentally that the pretransitional optical activity depends on the temperature as $(T-T^*)^{-0.5}$, where T^* is the metastability temperature of the isotropic phase. Two years later, Brazovskii and Dmitriev developed the first complete theory of phase transitions in cholesteric liquid crystals, and they predicted the existence of the blue phases [2]. The optical activity in the pretransitional region was derived using this approach by Dolganov *et al.* [3]. At this time, a detailed Landau theory of the cholesteric blue phases was obtained by Hornreich and Shtrikman, who also provided an outstanding study of the light scattering in the blue phases including a treatment of the polarization of the light, based on the formalism of the Müller matrices [4,5]. Bensimon, Domany, and Shtrikman studied the optical activity in the pretransitional regime and in the blue phases [6], confirming and extending the work of Dolganov. In their paper, the blue phase BP III was considered as an amorphous polycrystalline structure distinct from the isotropic phase, and their treatment of the optical activity relied on the long wavelength approximation. On the experimental side, the wavelength dependence of the optical activity in the blue phases was measured by Collings and co-workers [7,8]. The structure of BP III still remained mysterious until experiments clearly showed a continuous transition between BP III and the isotropic phase [9,10] and the existence of a critical point terminating a line of coexistence of the two phases [11]. In the same year, Lubensky and Stark developed a theory for the isotropic to BP III transition with a chiral liquid-gas-like critical point [12], which was extended to include scaling theory in Ref. [13]. Very recently, there has been a renewal of interest in the study of the blue phases with the discovery of the smectic blue phases [14], exhibiting isotropic–BP III coexistence terminating at a critical point [15].

In Sec. II of this paper, we introduce an effective index for the propagation of light in the isotropic phase and in BP III, which contains pretransitional effects such as the optical activity and the circular dichroism. In Sec. III, we present a derivation of these effects in a particular limit [6]. In Sec. IV, we make a digression on the optical properties of periodic chiral media for comparison with the case of nonperiodic chiral media. By evaluating our weak-scattering expression for the optical dielectric constant tensor in a cholesteric phase, we find the well-known de Vries formula, which describes the optical activity of light propagating in this medium along the pitch axis. In Sec. V we come back to isotropic chiral media and obtain the optical activity for arbitrary wavelength and chirality. This approach is different in that it is general, not limited to the long wavelength approximation, and applicable, in particular, to the resonant region where the wavelength of the light is of the order of the pitch of the cholesteric, a regime that has not been considered in detail in previous studies. In the long wavelength approximation, we collect contributions to the optical activity up to order $(P/\lambda)^4$. Though various contributions up to this order have appeared separately in the literature [2,3,6,16] and very recently in Ref. [17], these references are not fully consistent with each other. We, therefore, think that it is important to collect and discuss all these contributions in one place. We then generalize our method and obtain the wavelength dependence of the circular dichroism and of the symmetric part of the index, which to our knowledge have not appeared in the literature and have never been measured. Finally in Sec. VI, our theoretical predictions are sup-

ported by experimental spectra of the optical activity for different values of the chirality in the BP III phase [18]. The agreement between theory and experiments is very good. Experiments confirm the presence of a broad maximum in the magnitude of the optical activity when the wavelength is of the order of the pitch. This feature is the pretransitional signature in isotropic chiral media of the divergence arising from the long-range periodicity of the cholesteric phases is BP I and BP II.

II. THEORY

Let ϵ be the relative complex-valued dielectric constant of the cholesteric liquid crystal in the isotropic phase or in the blue phase BP III with respect to the average dielectric constant

$$\epsilon_{ij}(\mathbf{r}) = \delta_{ij} + \delta\epsilon_{ij}(\mathbf{r}), \tag{1}$$

where $\delta\epsilon_{ij}(\mathbf{r})$ is a relative anisotropic small local fluctuation of the dielectric constant: $\langle \delta\epsilon_{ij}(\mathbf{r})\rangle = 0, |\delta\epsilon_{ij}(\mathbf{r})| \ll 1$, and $\langle \cdots \rangle$ denotes a thermal average. To simplify the notations, we take the velocity of light in the medium to be 1, and we do not indicate explicitly the dependence of the dielectric constant on the frequency of light in the medium denoted ω. Maxwell equations in the absence of sources lead to the following Helmholtz equation for the electric field $\mathbf{E}(\mathbf{r},\omega)$:

$$\nabla \times [\nabla \times \mathbf{E}(\mathbf{r},\omega)] = \omega^2 \epsilon \cdot \mathbf{E}(\mathbf{r},\omega). \tag{2}$$

From Eq. (2), we deduce that the propagation of light in a homogeneous medium in the absence of fluctuations is characterized by the following Green's function:

$$G^0_{ij}(\mathbf{k},\omega) = \frac{\Delta_{ij}}{-\omega^2 + k^2 - i0^+} - \frac{k_i k_j}{\omega^2 k^2}, \tag{3}$$

where $\Delta_{ij} = \delta_{ij} - k_i k_j / k^2$ is a projector on the space transverse to the wave vector $\mathbf{k}$. The first term of Eq. (3) is the transverse part describing traveling wave solutions of Maxwell equations and the second term is the longitudinal part that describes nonpropagating modes. The scattering by the randomly fluctuating part of the dielectric function $\delta\epsilon_{ij}(\mathbf{r})$ is described by the following 4-rank tensor [19]:

$$B_{ijkl}(\mathbf{r}) = \omega^4 \langle \delta\epsilon_{ik}(\mathbf{r})\, \delta\epsilon_{jl}(0)\rangle. \tag{4}$$

Unless specified otherwise, we consider in this paper only nonabsorbing media in which the tensor $B_{ijkl}(\mathbf{r})$ is real. The averaged Green's function $G(\mathbf{k},\omega)$ follows from Dyson's equation,

$$G^{-1} = (G^0)^{-1} - \Sigma. \tag{5}$$

In the weak-scattering approximation, the tensor Σ can be calculated using the following equation [20]:

$$\Sigma_{ij}(\mathbf{k},\omega) = \int \frac{d^3\mathbf{q}}{(2\pi)^3} B_{ijkl}(\mathbf{q}) G^0_{kl}(\mathbf{k}-\mathbf{q},\omega), \tag{6}$$

in terms of the Fourier transform $B_{ijkl}(\mathbf{q})$ of the tensor defined in Eq. (4). Note that Eq. (6) is general and applies also to periodic media for which $B_{ijkl}(\mathbf{q})$ has δ-function peaks in which case this equation takes the form of a discrete sum over Bloch waves [21].

The general form of $\Sigma(\mathbf{k},\omega)$ in an isotropic chiral medium is

$$\Sigma_{ij}(\mathbf{k},\omega) = \Sigma_0(k,\omega)\,\delta_{ij} + \frac{i\epsilon_{ijl}k_l}{\omega}\Sigma_1(k,\omega) + \Sigma_2(k,\omega)\frac{k_i k_j}{\omega^2}. \tag{7}$$

If κ denotes a chiral parameter of the medium, $\Sigma_{ij}(\mathbf{k},\omega,\kappa)$ satisfy the general symmetry relation (valid in any medium in the absence of a magnetic field [22])

$$\Sigma_{ij}(\mathbf{k},\omega,\kappa) = \Sigma_{ji}(-\mathbf{k},\omega,\kappa), \tag{8}$$

and the chiral symmetry relation

$$\Sigma_{ij}(\mathbf{k},\omega,\kappa) = \Sigma_{ij}(-\mathbf{k},\omega,-\kappa). \tag{9}$$

The chiral symmetry relation implies that Σ_0 and Σ_2 are odd functions of κ and that Σ_1 is an even function of κ. The dispersion relation for light propagation modified by fluctuations is obtained from $\det[G_0^{-1}(\mathbf{k},\omega) - \Sigma(\mathbf{k},\omega)] = 0$. In a basis composed of two vectors perpendicular to $\mathbf{k}$, the diagonal elements of Σ are equal to Σ_0, and the off-diagonal elements are $\pm ik\Sigma_1/\omega$. In such a basis, the last term in Eq. (7) vanishes, and we find

$$\omega^2 - k^2 - \Sigma_0(k,\omega) = \pm\frac{k}{\omega}\Sigma_1(k,\omega). \tag{10}$$

This relation defines $k^+(\omega)$ and $k^-(\omega)$, which are respectively the dispersion relation for right and left circularly polarized light. Writing $k = \omega + \delta k$ and expanding Eq. (10) to first order in δk, one finds

$$\delta k^{\pm} = \frac{\Sigma_0(\omega,\omega) \pm \Sigma_1(\omega,\omega)}{-2\omega \mp \Sigma_1(\omega,\omega)/\omega \mp \partial\Sigma_1/\partial k - \partial\Sigma_0/\partial k}. \tag{11}$$

To first order in Σ, this gives $k^{\pm}(\omega) = \omega - [\Sigma_0(\omega,\omega) \pm \Sigma_1(\omega,\omega)]/2\omega$. The optical activity Φ is the angle through which the polarization vector of linearly polarized light has turned when traversing a medium of length L, thus $\Phi = \mathrm{Re}[k^+(\omega) - k^-(\omega)]L/2$. Similarly the circular dichroism, measuring the difference in transmission from left and right circularly polarized waves is $\Psi = \mathrm{Im}[k^+(\omega) - k^-(\omega)]L/2$. To first order in Σ, we have, therefore,

$$\Phi = \mathrm{Re}\frac{\Sigma_1(\omega,\omega)L}{2\omega}, \tag{12}$$

and

$$\Psi = \mathrm{Im}\frac{\Sigma_1(\omega,\omega)L}{2\omega}. \tag{13}$$

Note that these relations are valid at arbitrary frequency ω when Eq. (6) is valid. The fluctuations also modify the symmetric part of Σ, i.e., the average dielectric constant. The relative change of the average dielectric constant within the same approximation is $\Delta\epsilon_0 = -\Sigma_0(\omega,\omega)/\omega^2$.

We use in this paper the form of the Landau–de Gennes free energy of Ref. [5],

$$F = V^{-1}\int d^3\mathbf{r}\left\{\frac{1}{2}[a\epsilon_{ij}^2 + c_1\epsilon_{ij,l}^2 + c_2\epsilon_{ij,i}\epsilon_{lj,l} - 2de_{ijl}\epsilon_{in}\epsilon_{jn,l}] - \beta\epsilon_{ij}\epsilon_{jl}\epsilon_{li} + \gamma(\epsilon_{ij}^2)^2\right\}, \tag{14}$$

where $\epsilon_{ij,l} = \partial\epsilon_{ij}/\partial x_l$ and e_{ijk} is the Levi-Civita fully antisymmetric tensor. The coefficient a is proportional to the reduced temperature t, whereas all other coefficients are assumed to be temperature independent. As explained in Refs. [5,12], it is convenient to write this free energy in dimensionless form, by expressing all lengths in units of the order parameter correlation length $\xi_R = (12\gamma c_1/\beta^2)^{1/2}$. The chirality is then $\kappa_0 = q_c\xi_R$ where $q_c = d/c_1$ is the wave number of the cholesteric phase that determines the pitch $P = 4\pi/q_c$. The reduced temperature is defined by $t = (T - T_N^*)/(T_N - T_N^*)$ where T_N^* is the temperature corresponding to the limit of metastability of the isotropic phase [23] and $\rho = c_2/c_1$ is the ratio of the two Landau coefficients, which is of order 1. Using the Gaussian approximation for the fluctuations [6], the dielectric anisotropy correlation tensor defined in Eq. (4) takes the following form:

$$B_{ijkl}(\mathbf{q}) = \omega^4 \sum_{m=-2}^{m=2} \Gamma_m(q) T_{ik}^m(\hat{\mathbf{q}}) T_{jl}^{-m}(\hat{\mathbf{q}}), \tag{15}$$

where $\Gamma_m(q)$ is evaluated from the equipartition theorem

$$\Gamma_m(q) = \frac{k_B T}{t - m\kappa q + q^2\left[1 + \frac{\rho}{6}(4 - m^2)\right]}. \tag{16}$$

Note that q denotes the dimensionless wave vector measured in units of $1/\xi_R$ and that Eq. (16) has been corrected from the expression given in Ref. [12] (the factor $\rho/4$ has been replaced by $\rho/6$ in agreement with Ref. [5]). In Eq. (16), the parameter κ represents an effective chirality at the temperature t. Except at the critical point, κ is different from κ_0, and the difference $\kappa - \kappa_0$ is proportional to the order parameter of the BP III isotropic phase transition [12]. The index m in Eq. (15) denotes the five independent modes of the symmetric and traceless tensor $\delta\epsilon_{ij}(\mathbf{r})$. Note that Eq. (16) is equivalent to

$$\frac{k_B T}{\Gamma_m(q)} = t - m\kappa q + \Delta_m q^2 = \Delta_m(q - q_m)^2 + \tau_m, \tag{17}$$

with $\Delta_m = 1 + (\rho/6)(4 - m^2)$, $q_m = m\kappa/2\Delta_m$, $t_m = \Delta_m q_m^2$, and $\tau_m = t - t_m$. We have introduced t_m, the transition temperature of the mode m, and q_m, the wave vector that minimizes the energy of the mode m. Denoting $r = 1 + \rho/2$, we have explicitly $t_1 = t_{-1} = \kappa^2/4r$ and $q_1 = -q_{-1} = \kappa/2r$ for the modes ± 1; $t_2 = t_{-2} = \kappa^2$ and $q_2 = -q_{-2} = \kappa$ for the modes ± 2; $t_0 = 0$ and $q_0 = 0$ for the mode 0. A plot of $\Gamma_m(q)$ as a function of q is shown in Fig. 1 for the modes $m = 0,1$, and 2, a chirality $\kappa = 0.2$ and a temperature $t = 0.05$. This particular plot shows the dominance of the mode $m = 2$, because of the choice of the temperature $t > t_2 > t_1$ and t close to t_2. More generally it can be shown that as $t \to t_m$, $\Gamma_m(q)$ becomes a Dirac function localized at $q = q_m$.

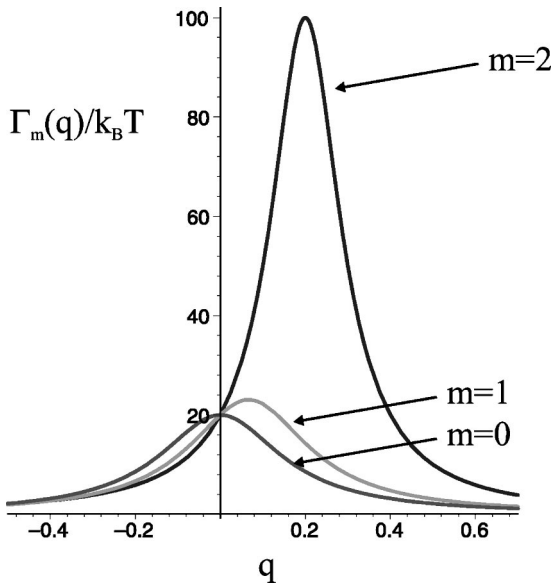

FIG. 1. Amplitude $\Gamma_m(q)/k_BT$ of the dielectric anisotropy correlation tensor as a function of the dimensionless wave vector q for the modes $m = 0,1$, and 2. κ is 0.2, $\rho = 1$, and the normalized temperature is $t = 0.05$.

The tensor T_{ij}^m introduced in Eq. (4) are eigenvectors of the tensor $B_{ijkl}(\mathbf{q})$, with eigenvalues $\omega^4\Gamma_m(q)$ [2]. These tensors are

$$T^0(\hat{\mathbf{q}}) = \frac{1}{\sqrt{6}}(3\hat{\mathbf{q}}\hat{\mathbf{q}} - 1), \tag{18}$$

$$T^1(\hat{\mathbf{q}}) = \frac{1}{\sqrt{2}}[\hat{\mathbf{q}}\mathbf{m}(\hat{\mathbf{q}}) + \mathbf{m}(\hat{\mathbf{q}})\hat{\mathbf{q}}] = T^{-1}(\hat{\mathbf{q}})^*, \tag{19}$$

$$T^2(\hat{\mathbf{q}}) = \mathbf{m}(\hat{\mathbf{q}})\mathbf{m}(\hat{\mathbf{q}}) = T^{-2}(\hat{\mathbf{q}})^*, \tag{20}$$

with $\mathbf{m} = (1/\sqrt{2})(\hat{\boldsymbol{\xi}} + i\hat{\boldsymbol{\eta}})$ and $(\hat{\boldsymbol{\xi}}, \hat{\boldsymbol{\eta}}, \hat{\mathbf{q}})$ forming a right-handed system of orthonormal vectors. We choose the vectors $\hat{\boldsymbol{\xi}}$ and $\hat{\boldsymbol{\eta}}$ such that $\hat{\boldsymbol{\xi}}(-\hat{\mathbf{q}}) = \hat{\boldsymbol{\xi}}(\hat{\mathbf{q}})$ and $\hat{\boldsymbol{\eta}}(-\hat{\mathbf{q}}) = -\hat{\boldsymbol{\eta}}(\hat{\mathbf{q}})$, so that

$$\mathbf{m}(-\hat{\mathbf{q}}) = \mathbf{m}(\hat{\mathbf{q}})^*. \tag{21}$$

III. DISPERSION EFFECTS IN THE LIMIT $k \to 0$

In this section the optical activity and the circular dichroism of isotropic chiral media is derived using the method of Ref. [6]. This method gives the optical activity as an expansion in powers of ω for $k \to 0$. As we shall see later, this limit does not correspond to the physical limit of the optical activity in the long wavelength approximation, but we present this derivation here for pedagogical purposes. The physical limit of the optical activity in the long wavelength approximation together with an exact analytical expression for the optical activity at arbitrary wavelength will be presented in Sec. V. Following Ref. [6], we use an expansion to first order in $\mathbf{k}$ of the Green's function

$$G^0_{ij}(\mathbf{k}-\mathbf{q},\omega) \simeq G^0_{ij}(\mathbf{q},\omega) - k_l \frac{\partial G^0_{ij}(\mathbf{q},\omega)}{\partial q_l}, \tag{22}$$

with

$$\frac{\partial G^0_{ij}(\mathbf{q})}{\partial q_l} = -\frac{q_i \Delta_{jl} + q_j \Delta_{il}}{\omega^2(\omega^2 - q^2 + i0^+)} + \frac{2q_l \Delta_{ij}}{(\omega^2 - q^2 + i0^+)^2}. \tag{23}$$

Using this expression in Eq. (6), we obtain $\Sigma_1(k \to 0, \omega)$, which was defined in Eq. (7). After integration over $\mathbf{q}$, we obtain

$$\Sigma_1(k \to 0, \omega) = \int dq q^2 \frac{\omega^3 q[-\Omega_1(q)\omega^2 + \Omega_1(q) q^2 - 2\,\Omega_2(q)\omega^2]}{12\pi^2(\omega^2 - q^2 + i0^+)^2}, \tag{24}$$

where $\Omega_m(q) = \Gamma_m(q) - \Gamma_{-m}(q)$. In the integration of Eq. (24), we take the upper limit of integration over q to be infinity. The continuous model used in this paper is valid only up to wave vectors $q_{max} = 2\pi/a$, where a is an intermolecular distance, but in the case of Eq. (24), the integral is not sensitive to the value of q_{max} as discussed in Refs. [3,12].

Expanding Eq. (24) in powers of ω, and integrating over q, we obtain the complex-valued $\Sigma_1(k \to 0, \omega)$ in powers of ω for $k \to 0$. Using Eqs. (12) and (13), the optical activity is in this limit

$$\frac{\Phi}{L} = \frac{\kappa\,\omega^2 k_B T}{48 r^{3/2}\sqrt{\tau_1}\pi} + \left(\frac{1}{4\sqrt{r}\,\tau_1^{3/2}} - \frac{1}{\tau_2^{3/2}}\right)\frac{\omega^4 k_B T \kappa}{12\pi} \tag{25}$$

and the circular dicroism

$$\frac{\Psi}{L} = \left(-\frac{1}{\tau_2^2} + \frac{1}{6\,\tau_1^2}\right)\frac{\omega^5 k_B T \kappa}{4\pi}. \tag{26}$$

Deriving Eqs. (25) and (26), we have assumed that $\kappa \ll \sqrt{\tau_2}$ and $\kappa \ll \sqrt{4r\tau_1}$, and the equations are valid for temperatures such that $t_1 < t_2 < t$. Within these approximations, the optical rotation and circular dichroism are proportional to the chirality κ. The next order will be of order κ^3 as imposed by the symmetry relation of Eq. (9).

IV. de VRIES FORMULA

We present in this section a derivation of the de Vries formula, which is the well-known solution of Maxwell's equations for light propagating in a cholesteric liquid crystal along the pitch axis [27]. The reason of this digression into the optics of periodic chiral media will become clear in the following section, where we explore the relation between optical activity in isotropic chiral liquid crystals and the de Vries formula for the cholesteric phase. We shall take the z axis to be the helical axis of the cholesteric phase and $(\hat{\mathbf{e}}_x, \hat{\mathbf{e}}_y, \hat{\mathbf{e}}_z)$ to be a right-handed frame. In the cholesteric phase, the order parameter, the anisotropy in the dielectric constant, is

$$\delta\epsilon_{ij} = \epsilon_a\left(n_i n_j - \frac{1}{3}\delta_{ij}\right), \tag{27}$$

where $\epsilon_a = \epsilon_\parallel - \epsilon_\perp$ and $n = \cos(\kappa z/2)\hat{\mathbf{e}}_x + \sin(\kappa z/2)\hat{\mathbf{e}}_y$. Using Eq. (27) and the definitions (18)–(20), it is simple to show that

$$\delta\epsilon_{ij}(\mathbf{r}) = \delta\epsilon_{ij}(z) = \frac{\epsilon_a}{2}[e^{i\kappa z} T^{-2}_{ij}(\hat{\mathbf{e}}_z) + e^{-i\kappa z} T^{2}_{ij}(\hat{\mathbf{e}}_z)] - \frac{\epsilon_a}{\sqrt{6}} T^0_{ij}(\hat{\mathbf{e}}_z). \tag{28}$$

From this, the tensor $B_{ijkl}(\mathbf{r}) = B_{ijkl}(z)$ defined in Eq. (4) can be constructed. To calculate its Fourier transform $B_{ijkl}(\mathbf{q})$, it is convenient to use a spherical coordinate system with $\mathbf{q} = q(\sin\theta\cos\phi, \sin\theta\sin\phi, \cos\theta)$,

$$B_{ijkl}(\mathbf{q}) = \omega^4 \int dx \exp[iq\sin\theta\cos\phi x] \int dy \exp\Big[iq\sin\theta\sin\phi y \times \int dz \exp[iq\cos\theta z]\,\delta\epsilon_{ik}(z)\,\delta\epsilon_{jl}(0), \tag{29}$$

which can be simplified using Eq. (28)

$$\begin{aligned} B_{ijkl}(\mathbf{q}) &= \frac{\omega^4 \epsilon_a^2 (2\pi)^3}{4q^2\sin\theta}\delta(\phi)\,\delta(\theta)[\,\delta(q+\kappa) T^{-2}_{ik} T^2_{jl} \\ &\quad + \delta(q-\kappa) T^2_{ik} T^{-2}_{jl}] + A_{ijkl}(\mathbf{q}), \\ &= \frac{\omega^4 \epsilon_a^2 (2\pi)^3}{4}[\,\delta^3(\mathbf{q} + \kappa\hat{\mathbf{e}}_z) T^{-2}_{ik} T^2_{jl} \\ &\quad + \delta^3(\mathbf{q} - \kappa\hat{\mathbf{e}}_z) T^2_{ik} T^{-2}_{jl}] + A_{ijkl}(\mathbf{q}), \end{aligned} \tag{30}$$

where $T^{\pm 2}_{ij} = T^{\pm 2}_{ij}(\hat{\mathbf{e}}_z)$ and A_{ijkl} is a linear combination of tensors of the form $T^m_{ik} T^{m'}_{jl}$ with m and m' being 0,2, or

-2. The Bragg peaks of the cholesteric phase located at $\mathbf{q}=\pm\kappa\hat{\mathbf{e}}_z$ correspond to the first two terms of Eq. (30). Note that in a periodic medium considered in this section, Σ_1 is a function of $\mathbf{k}$, whereas in an isotropic medium to be considered in the following section, Σ_1 is only a function of $k=|\mathbf{k}|$. In a periodic medium $\Sigma_1(\mathbf{k},\omega)$ can be derived generally from $\Sigma_{ij}(\mathbf{k},\omega)$ using

$$\frac{\Sigma_1(\mathbf{k},\omega)}{\omega}=\frac{[\Sigma_{ij}(\mathbf{k},\omega)-\Sigma_{ij}(-\mathbf{k},\omega)]e_{ijl}k_l}{4ik^2}. \tag{31}$$

Using Eqs. (6), (30), and (31), we find

$$\frac{\Sigma_1(\mathbf{k},\omega)}{\omega}=\frac{\omega^4\epsilon_a^2 e_{ijm}k_m}{16ik^2}[G^0_{kl}(\mathbf{k}+\kappa\hat{\mathbf{e}}_z)-G^0_{kl}(-\mathbf{k}+\kappa\hat{\mathbf{e}}_z)] \times[T^{-2}_{ik}T^2_{jl}-T^2_{ik}T^{-2}_{jl}+\tilde{A}_{ijkl}], \tag{32}$$

where $\tilde{A}_{ijkl}=(-T^{-2}_{ik}+T^2_{ik})T^0_{jl}/\sqrt{6}$. In Eq. (32), the tensors T can be eliminated using Eqs. (18) and (20).

We now assumes that $\mathbf{k}$ is along the z axis. In this case, it is simple to show that the tensor $\tilde{A}_{ijkl}$ does not contribute to Σ_1. According to the analysis of Sec. II, to linear order in Σ the optical activity and the circular dichroism are proportional to the real and imaginary part of $\Sigma_1(\mathbf{k},\omega)$ evaluated at $|\mathbf{k}|=\omega$. With these assumptions, Eq. (32) gives

$$\frac{\Sigma_1(\mathbf{k}=\omega\hat{\mathbf{e}}_z,\omega)}{\omega}=\frac{\omega^4\epsilon_a^2\kappa}{(\kappa^2+2\omega\kappa-i0^+)(2\omega\kappa-\kappa^2+i0^+)}. \tag{33}$$

The real part of Eq. (33) leads to the de Vries formula [27]

$$\frac{\Phi}{L}=\frac{\pi\epsilon_a^2}{16P\lambda'^2[1-\lambda'^2]}, \tag{34}$$

where $\lambda'=\lambda/P$ and $P=4\pi\xi_R/\kappa$, the pitch of the cholesteric phase, and the circular dichroism Ψ is zero within the same approximations. Note the following features [27]: there is a dispersion anomaly at the Bragg reflection $\lambda'=1$, but both Eq. (34) and $\Psi=0$ break down near the Bragg reflection. Indeed close to the Bragg reflection, terms of higher order in Σ contribute to the optical rotation and the circular dichroism, and for this reason Eqs. (34) and $\Psi=0$ are only valid in the domain $\epsilon_a\lambda\ll||P|-\lambda|$ [28]. The sign of the optical rotation is such that a right-handed helix ($\kappa>0$) produces a positive optical rotation (the material is laevogyric) when $\lambda\ll P$ and a negative one (the material is dextrogyric) when $\lambda\gg P$. In the long wavelength limit $\lambda\ll P$, the de Vries optical activity Φ/L is of order P^3/λ^4 and depends on the light propagation direction as opposed to the isotropic–BP III phases where it is of order P/λ^2 and is independent of the light propagation direction.

V. WAVELENGTH DEPENDENCE OF SPATIAL DISPERSION EFFECTS IN AN ISOTROPIC CHIRAL MEDIUM

In this section, we compute the exact wavelength dependance of the optical activity, the circular dichroism and the average index in an isotropic chiral medium, without relying on the long wavelength approximation and at any order in the chirality κ. The method has been pioneered by Dolganov and co-workers [3,16] in their studies of BP I and BP II, but this reference does not present all the details of the calculation. Instead of using the expansion Eq. (22), which is only valid in the long wavelength approximation, we calculate exactly $\Sigma_1(k,\omega)$ from Eqs. (6) and (31). Separating the contribution from the modes $m=2$ and $m=1$, we obtain (see Appendix A for details)

$$\frac{\Sigma_1^{m=\pm2}(k,\omega)}{\omega}=\int\frac{d^3\mathbf{q}}{(2\pi)^3}\frac{\mp q\omega^2c^2\Gamma_{\pm2}(q)(2\omega^2-k^2+k^2c^2)}{2(k^2+2kqc+q^2-\omega^2-i0^+)(k^2-2kqc+q^2-\omega^2-i0^+)}, \tag{35}$$

and

$$\frac{\Sigma_1^{m=\pm1}(k,\omega)}{\omega}=\int\frac{d^3\mathbf{q}}{(2\pi)^3}\frac{\mp q\omega^2\Gamma_{\pm1}(q)(c^2-1)(\omega^2+4k^2c^2-k^2-q^2)}{4(k^2+2kqc+q^2-\omega^2-i0^+)(-k^2+2kqc-q^2+\omega^2+i0^+)}, \tag{36}$$

with $c=\hat{\mathbf{k}}\cdot\hat{\mathbf{q}}$. From these equations, the contribution of the modes $m=\pm1$ and $m=\pm2$ of Eq. (24) of Sec. III is recovered in the limit $\mathbf{k}\to0$. According to the analysis of Sec. II, however, the correct procedure to obtain the optical activity and the circular dichroism to leading order in Σ is from $\Sigma_1(k,\omega)$ evaluated at $k=\omega$. As will become clear later, this does not give the same result, in general, when compared to Sec. III where the limit $\mathbf{k}\to0$ is taken in Eq. (22). Using $k=\omega$, Eqs. (35) and (36) can be simplified,

$$\frac{\Sigma_1^{m=\pm2}(\omega,\omega)}{\omega} =\int\frac{d^3\mathbf{q}}{(2\pi)^3}\frac{\mp\omega^4c^2\Gamma_{\pm2}(q)(1+c^2)}{2(q+2\omega c-i0^+)(q-2\omega c-i0^+)q} \tag{37}$$

and

$$\frac{\Sigma_1^{m=\pm 1}(\omega,\omega)}{\omega}=\int \frac{d^3\mathbf{q}}{(2\pi)^3}\frac{\mp\omega^2\Gamma_{\pm 1}(q)}{4q}(c^2-1). \quad (38)$$

Note that the integrand of Eq. (38) vanishes for $\mathbf{k}\|\mathbf{q}$ but is nonzero otherwise. This means that the modes $m=\pm 1$ contribute only if the light is propagating off axis or if the pitch axis and the director are not perpendicular to each other as in smectic C^* for instance. Equation (37) is the analog for isotropic chiral media of the de Vries formula of Eq. (33) valid for periodic media. The two expressions become identical with the replacements $c\to 1$ since the light is propagating along the pitch axis and $q\to\pm\kappa$ according to Eq. (30). Other periodic and chiral media such as BP I and BP II can be treated as the cholesteric phase in Sec. IV. Therefore, we expect in BP I and BP II a divergence of the $m=\pm 2$ contribution to the optical activity at the Bragg condition, i.e., when the denominator of Eq. (37) is zero, and a change of sign of the optical activity when crossing this point. There should be no divergence for the modes $m=\pm 1$ as can be inferred from Eq. (38).

The recent reference of Hunte and Singh [17] contains a derivation of the pretransitional optical activity in isotropic chiral media, which uses a method similar to the one presented in this paper although the authors have only applied it to the long wavelength regime. We believe that the authors have made an error in deriving Eqs. (30) and (31) of Ref. [17] that represent, respectively, the contribution of the modes $m=\pm 1$ and $m=\pm 2$ to the optical activity. The integrand of Eq. (30) of Ref. [17] should vanish when $c=1$ as is true for the integrand of Eq. (38) but it does not, and Eq. (31) of Ref. [17] should reproduce the de Vries as is true for Eq. (37) but does not. Therefore, we think that the results of the derivation of the optical activity in Ref. [17] are incorrect although the method used is valid.

A straightforward evaluation of Eq. (38) gives Σ_1 for the modes $m=\pm 1$ and for an arbitrary frequency ω,

$$\frac{\Sigma_1^{m=\pm 1}(\omega,\omega)}{\omega}=\frac{\omega^2\kappa k_B T}{24\pi r^{3/2}\sqrt{\tau_1}}. \quad (39)$$

The $m=\pm 1$ contribution of the optical activity has a trivial frequency dependence of ω^2. The reason is the following: the modes $m=\pm 1$ have the property that $T^{\pm 1}(\hat{\mathbf{q}})\cdot\hat{\mathbf{q}}\neq 0$ whereas $T^{\pm 2}(\hat{\mathbf{q}})\cdot\hat{\mathbf{q}}=0$ for the modes $m=\pm 2$. Using Eq. (6), this property implies the following selection rule: the $m=\pm 1$ contribution to the optical activity in the long wavelength limit is related to the longitudinal part of the Green's function (also called near-field part), which is the second term in the right-hand side of Eq. (3). The only pole of the near-field Green's function is at $\omega=0$, which is the reason for the absence of a complex wavelength dependence for the modes $m=\pm 1$ and also the reason for which these modes give the leading contribution to the optical activity at small ω.

Therefore, the most interesting part of the wavelength dependence of the optical activity comes from the modes $m=\pm 2$. It is also the dominant contribution when t is close to t_2. The integration in Eq. (37) can be done analytically for $t>t_2$, and the final result (see Appendix B for details of the derivation) is

$$\mathrm{Re}\frac{\Sigma_1^{m=\pm 2}(\omega,\omega)}{\omega}=\frac{-\omega^3}{32\pi\sqrt{\tau_2}}[x_1 f(x_1)-x_3 f(x_3)]k_B T, \quad (40)$$

where $x_1=(\kappa+i\sqrt{\tau_2})/2\omega$ and $x_3=(-\kappa+i\sqrt{\tau_2})/2\omega$. Note that Eq. (40) agrees with the symmetry relation of Eq. (9). We have introduced the function

$$f(x)=-2x^2-\frac{8}{3}+(x+x^3)\ln\left(\frac{x+1}{x-1}\right). \quad (41)$$

This function tends to $-8/3$ as $x\to\infty$, is equivalent to $16/15x^2$ as $x\to 0$, and diverges at $x=\pm 1$ as a result of the divergence of the initial expression of Eq. (37). Equations (40) and (41) fully agree with Filev's results in Ref. [24] quoted for $\tau_2=0$. Similar functions but not exactly identical functions are present in Refs. [2,16,17,29], which could indicate misprints or errors regarding this particular point.

A. The long and the short wavelength limits

It is interesting to consider two particular cases of Eq. (40), the case where $\omega\ll\kappa$, which defines the long wavelength limit and the opposite case where $\omega\gg\kappa$ the short wavelength limit. In the first case, it is easy to deduce from Eq. (40) that $\mathrm{Re}\Sigma_1^{m=\pm 2}(\omega,\omega)/\omega=-2\omega^4\kappa k_B T/15\pi\sqrt{\tau_2}t$. Therefore, the optical activity in the long wavelength approximation for a temperature $t>t_2>t_1$ is

$$\frac{\Phi}{k_B T L}=\frac{\omega^2\kappa}{48\pi r^{3/2}\sqrt{\tau_1}}-\frac{\omega^4\kappa}{15\pi\sqrt{\tau_2}t}+o(\omega^4). \quad (42)$$

Note that Eq. (42) is not identical with Eq. (25) because $\lim_{\omega\to 0}\Sigma(\omega,\omega)\neq\lim_{k\to 0}\Sigma(k,\omega)$. Therefore, Eq. (42) is the physical limit of the optical activity in the long wavelength approximation whereas Eq. (25) is not. The first term in Eq. (42) is identical to the expression of Refs. [3,6] for the optical activity in the pretransitional region. It is associated with the modes $m=\pm 1$ and gives the $(T-T_1^*)^{-0.5}$ dependence observed in many experiments. As first noted by Filev, the modes $m=\pm 2$ need to be considered in addition to the modes $m=\pm 1$, in a region very close to the transition in highly chiral liquid crystals [24]. This is the origin of the second term in Eq. (42), whose contribution has the opposite sign with respect to the contribution from the $m=\pm 1$ modes. Therefore, there is a competition between these two modes, which leads to a maximum in the optical activity as a function of the temperature t as shown in Fig. 2 for a chirality $\kappa=0.2$. There has been some debate in the literature concerning the temperature dependence of this term, whether it should be in $(T-T_2^*)^{-1/2}$ as predicted in Eq. (42) or in $(T-T_2^*)^{-3/2}$ as predicted by other approaches such as the one that gives Eq. (25). The very short paper of Ref. [24] did not provide enough explanations to answer this point, and that of Ref. [16] also lacks explanations and contains some errors or

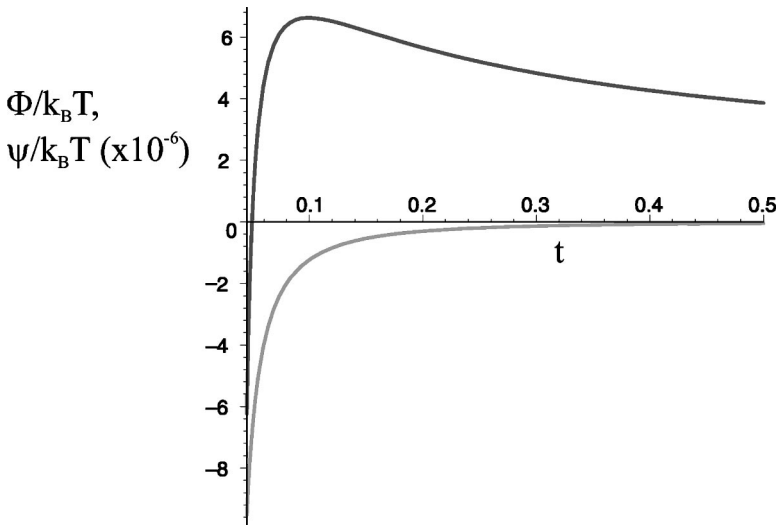

FIG. 2. Optical activity Φ/Lk_BT, the dark curve, and circular dichroism Ψ/Lk_BT, the light curve as a function of the temperature t for $\kappa=0.2$. The wavelength is $\lambda=100\xi_R$, which corresponds to the long wavelength regime where Eq. (42) is applicable. The curve of the optical activity illustrates the competition between the modes $m=\pm1$ and $m=\pm2$, the latter being responsible for the decrease (and the change of sign) of the optical activity when t approaches t_2.

misprints [in particular, in Eq. (4) of Ref. [16]]. In Ref. [25], Collings and co-workers studied experimentally systems of high chirality and found good agreement with Filev's model with a 1/2 exponent. Unfortunately due to a large number of fitting parameters, the data could also have been explained with an exponent $-3/2$ [7]. In a study of the wavelength dependence of the optical activity in the long wavelength regime [8], Collings and co-workers confirmed that the modes $m=\pm2$ contribute to higher order than the modes $m=\pm1$ in agreement with Eq. (42). According to Eq. (42), there should be no second order correction in ω^4 for the modes $m=\pm1$ with a dependence $(T-T_1^*)^{-3/2}$, as was incorrectly predicted in Eq. (25). This point could not be proved or disproved experimentally, because quite good fits to the data can be obtained with or without this term included as found in Refs. [17,26]. In the short wavelength limit $\omega \gg \kappa$, we find using Eq. (40) that $\mathrm{Re}\Sigma_1^{m=\pm2}(\omega,\omega)/\omega = \omega^2\kappa k_BT/12\pi\sqrt{\tau_2}$.

B. The resonance region

We now consider the complete wavelength dependence of the optical activity for the modes $m=\pm2$. In Figs. 3(a) and 3(b), the optical activity and the circular dichroism are shown as a function of the wavelength expressed in units of ξ_R, as calculated with Eqs. (40) and (B5). In Fig. 3(a) $\tau_2=10^{-3}$ and in Fig. 3(b) $\tau_2=10^{-5}$. Note that in all these figures, a positive value of κ has been chosen corresponding to a right-handed helix in the cholesteric phase, but that an opposite optical activity and circular dichroism would have been found with a left-handed helix. These figures clearly show a maximum in the magnitude of the optical activity when the wavelength is equal to the pitch P of the cholesteric phase, which is about $62.8\xi_R$ for $\kappa=0.2$ in the case of Fig. 3. This maximum at this wavelength is the remains in the isotropic phase of the divergence present in the optical activity of BP I and BP II and in the de Vries formula in Eq. (34). As t gets closer to t_2, $\Gamma_2(q)$ becomes peaked at $q=\kappa$, and the width of the maximum in the magnitude of the optical activity gets smaller as can be seen by comparing Figs. 3(a) and 3(b).

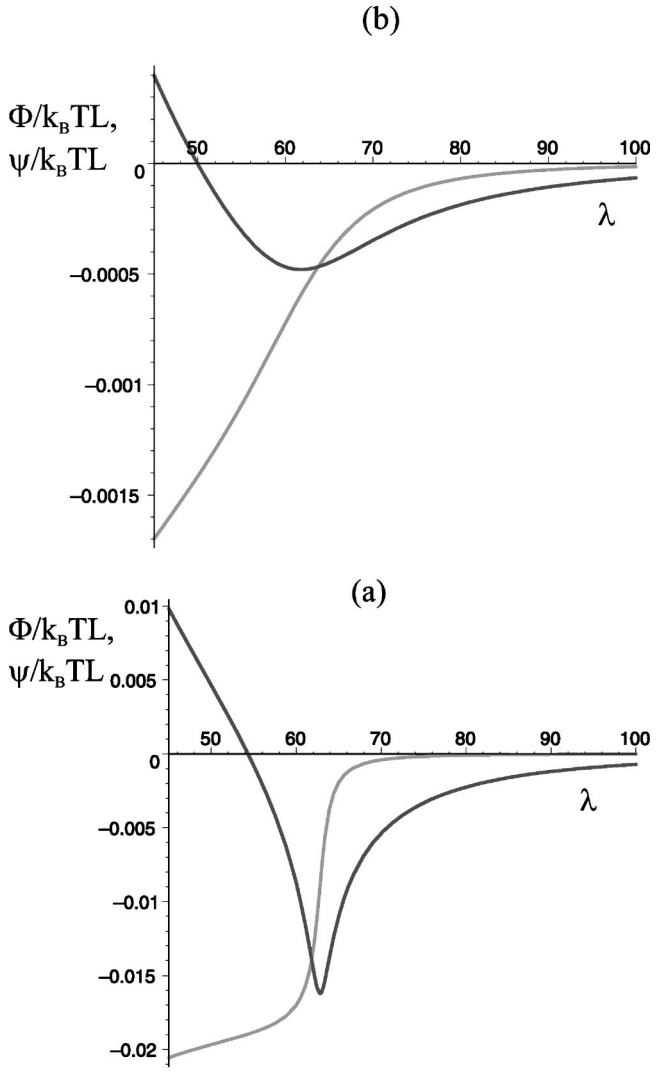

FIG. 3. The contribution from the modes $m=\pm2$ to the optical activity Φ/Lk_BT, the dark curve, and the circular dichroism Ψ/Lk_BT, the light curve, are shown as a function of the wavelength λ for $\kappa=0.2$. (a) The temperature t is such that $\tau_2=10^{-5}$ and (b) $\tau_2=10^{-3}$. The optical activity is the darker curve and the wavelength is expressed in units of $\xi_R=25$ nm.

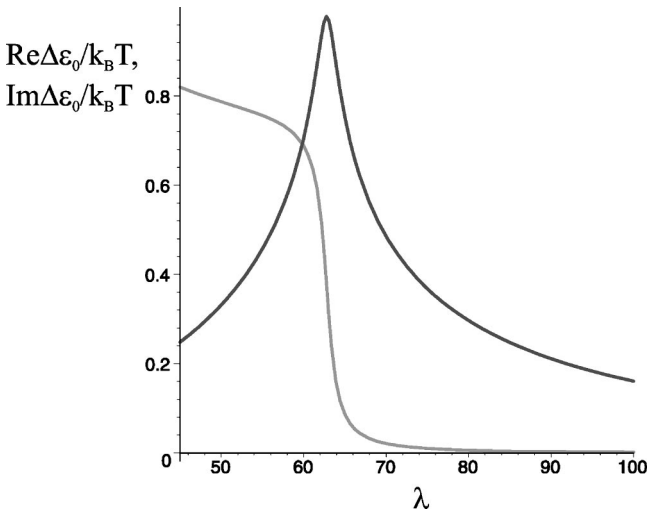

FIG. 4. Real (in dark) and imaginary (in light) part of the $m=\pm 2$ contribution to the average dielectric constant $\Delta\epsilon_0$ as a function of the wavelength that is expressed in units of $\xi_R=25$ nm. Note that $\kappa=0.2$ and $\tau_2=10^{-5}$.

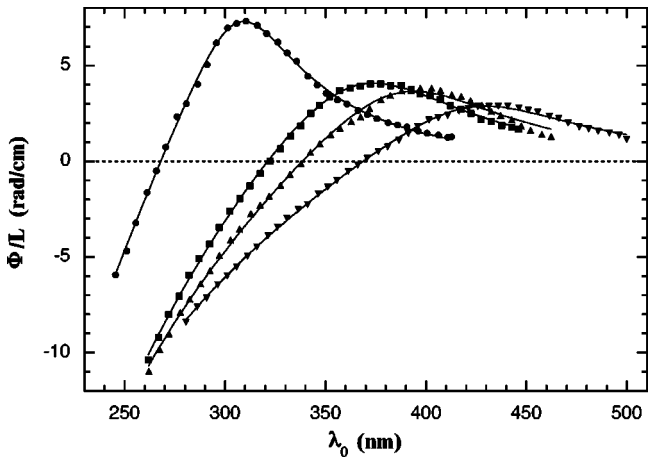

FIG. 5. Measured ORD spectra (points) in the BP III phase as a function of the wavelength of light in vacuum λ_0, together with a fit (solid curve) using Eqs. (39) and (40). The ORD spectra are shown for pure cholesteryl myristate (CM) with circles, for pure cholesteryl nonanoate (CN) with squares, for mixtures of CN with 5 and 10 mol % of cholesteryl chloride (CC) with upper and lower triangles, respectively.

C. Circular dichroism and average dielectric constant

These figures also show the circular dichroism, which to our knowledge has never been discussed theoretically or measured directly in isotropic chiral media. The absence of experiments is probably due to the difficulty separating the contribution from pretransitional fluctuations and the contribution from the absorption bands. According to Fig. 3, circular dichroism is best observed in the region where $\omega \gg \kappa$ as it gets very small when $\omega \ll \kappa$. The curve shown in the figure is the contribution from pretransitional fluctuations, which is valid away from absorption bands. Note that experimentally this circular dichroism translates in the multiple light scattering regime into a difference in the scattering mean-free paths for circularly polarized waves. This means that the transport properties of light in the multiple light scattering regime should be different for the different states of circular polarization. Such a difference has indeed been observed in static and dynamic light scattering measurements with circularly polarized light in the isotropic phase and in BP III [30].

Finally we have applied our method to the modification of the average dielectric constant due to the fluctuations. In Sec. II, we have defined this quantity as $\Delta\epsilon_0=-\Sigma_0(\omega,\omega)/\omega^2$, where Σ_0 is the isotropic part of Σ. The effect of the fluctuations on the symmetric part of the dielectric constant has to our knowledge never been calculated or measured in the pretransitional region. We find that all the five modes contribute to this average dielectric constant. In order to illustrate a case where the corrections can be large, we focus here on the contribution of the modes $m=\pm 2$, which as noted before is dominant when t is sufficiently close to t_2. Using Eqs. (6) and (7), we find

$$\Sigma_0^{m=\pm 2}(\omega,\omega)=\frac{\omega^4}{2(2\pi)^3}\int d^3\mathbf{q}\frac{(1+c^2)\Lambda_2(q)}{2q\omega c-q^2+i0^+}, \quad (43)$$

with $\Lambda_2(q)=\Gamma_2(q)+\Gamma_{-2}(q)$. After integrating over c and q, one obtains

$$\mathrm{Re}\Delta\epsilon_0^{m=\pm 2}=\frac{\omega^3}{64\pi\sqrt{\tau_2}\kappa}[g(x_1,t)-g(x_3,t)]k_BT, \quad (44)$$

with

$$g(x,t)=-\frac{t+(2\omega x)^2}{\omega^2}\left[(1+x^2)\ln\left(\frac{-1+x}{1+x}\right)+2x\right], \quad (45)$$

and

TABLE I. Parameters of the fit of the optical activity spectra for the different samples: pure cholesteryl myristate (CM), pure cholesteryl nonanoate (CN), and mixtures of CN with 5 and 10 mol % of cholesteryl chloride (CC).

	A_1 (rad nm^2)	A_2 (nm^{-1})	A_3 (nm^{-1})	A_4 (rad nm)
CM	$-(1.62\pm0.26)$	$(4.90\pm0.03)\times10^{-3}$	$(4.28\pm0.99)\times10^{-4}$	$-(5.54\pm2.11)\times10^{-3}$
CN	$-(2.45\pm0.38)$	$(3.99\pm0.05)\times10^{-3}$	$(5.24\pm1.17)\times10^{-4}$	$-(8.41\pm1.51)\times10^{-3}$
CN/5CC	$-(2.31\pm0.32)$	$(3.79\pm0.05)\times10^{-3}$	$(4.45\pm1.00)\times10^{-4}$	$-(7.24\pm1.31)\times10^{-3}$
CN/10CC	$-(2.19\pm0.35)$	$(3.46\pm0.06)\times10^{-3}$	$(3.76\pm1.05)\times10^{-4}$	$-(5.91\pm1.43)\times10^{-3}$

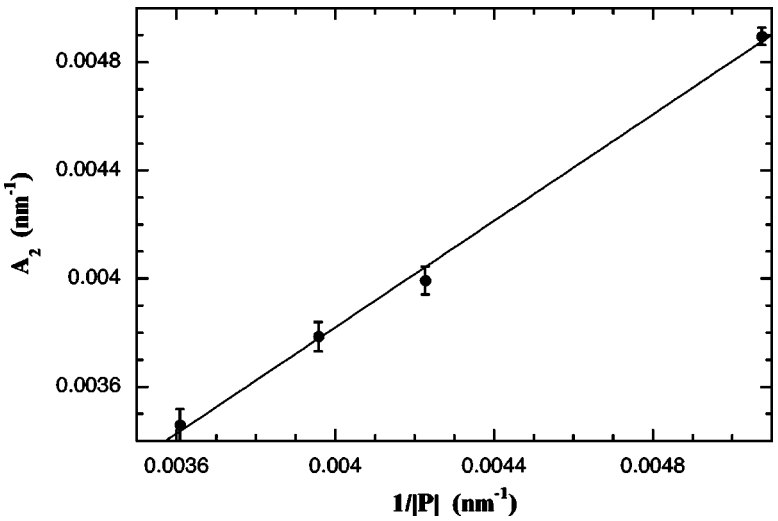

FIG. 6. Chirality parameter A_2 deduced from the fit of Fig. 5 as a function of the absolute value of the inverse pitch of the cholesteric phase $1/|P|$.

$$\mathrm{Im}\Delta\epsilon_0^{m=\pm 2}=\frac{\omega^3}{4\pi}\int_0^1 (1+x^2)x\,dx\,\Lambda_2(2\omega x). \qquad (46)$$

As imposed by the symmetry relation of Eq. (9), $\Delta\epsilon_0$ of Eq. (44) is an even function of κ. In Fig. 4, the real and imaginary part of the average dielectric constant $\Delta\epsilon_0$ is shown as a function of the wavelength, as calculated using Eqs. (44) and (46) for the modes $m=\pm 2$. Similarly to the case of the optical activity, there is a maximum in $\Delta\epsilon_0$ as a function of the wavelength when the wavelength is of the order of the pitch of the cholesteric.

VI. THEORY VS EXPERIMENT

In this section, we compare the prediction of our model with optical rotary dispersion (ORD) measurements, in the BP III phase taken from Ref. [18]. This reference is the only one known to us that reports measurements of the optical activity in the isotropic phase and in BP III beyond the long wavelength regime. The ORD spectra are measured in the BP III phase for pure cholesteryl myristate (CM), pure cholesteryl nonanoate (CN), and mixtures of CN with small quantities of cholesteryl chloride (CC), a compound of opposite chirality. The sign of the optical rotation agrees with Sec. IV: all the samples have a dominant left-handed character ($\kappa<0$ and $P<0$), and the optical activity is indeed found to be negative when $\lambda \ll |P|$. The optical activity presents a broad maximum at $\lambda \simeq -P$, which grows smaller and broader and shifts to higher wavelength as $|P|$ is increased. The curves are fitted with a theoretical expression, which is the sum of Eq. (39) (for the modes $m=\pm 1$) and Eq. (40) (for the modes $m=\pm 2$), and as can be seen in Fig. 5, the fits are excellent. The spatial dispersion of the index, which affects the wavelength of the light in the medium λ, is incorporated in this fit using the measurements on CN reported in Ref. [31]. There are four free parameters in this fit, A_1, A_2, A_3, and A_4. These parameters are $A_1=\pi^2 k_B T \xi_R^3/8\sqrt{\tau_2}$, $A_2=-\kappa/4\pi\xi_R=1/|P|$, $A_3=\sqrt{\tau_2}/4\pi\xi_R$, and $A_4=\kappa k_B T \xi_R^2 \pi/12\sqrt{\tau_1} r^{3/2}$ so that $x=(\pm A_2+iA_3)\lambda$, where λ is expressed in nanometers and A_2 and A_3 have units of nm^{-1}. The values of these parameters for the different samples are shown in Table I. The parameter A_2 obtained from the fits should be identical to the absolute value of the inverse pitch of the cholesteric phase. This is indeed the case as shown in Fig. 6, where the points correspond to the measurements of Fig. 5 and the solid line is a linear fit that gives a slope of 0.98 ± 0.04 and an intercept of $(-1.2\pm 1.6)\times 10^{-4}$.

VII. CONCLUSION

In this paper, we have discussed spatial dispersion effects (optical activity, circular dichroism, and average index) for light propagation in the isotropic–BP III phase, by introducing an effective index that describes the fluctuations. We have obtained the wavelength dependence of the spatial dispersion effects without relying on the long wavelength approximation, on which previous studies on this problem have been based. This approach allows us to discuss the optical properties in the resonant region when the wavelength of the light is of the order of the pitch of the cholesteric. In the vicinity of this point, there is a divergence of the magnitude of the optical activity in the cholesteric, BP I and BP II phases and a broad maximum in the case of the BP III and isotropic phases. These features are confirmed by measurements of spectra of the optical activity in the BP III phase for different values of the chirality. We have also provided predictions for the wavelength dependence of the circular dichroism and for the symmetric part of the effective index. We hope that this work will motivate experimentalists to study the optical properties of periodic and nonperiodic chiral media.

ACKNOWLEDGMENTS

We acknowledge many stimulating discussions with B. Pansu, P. Ziherl, and P. Galatola. This work was supported in part by the MRSEC program under Grant No. NSF DMR00-79909. D.L. received support by a grant from the French Ministry of Foreign Affairs.

APPENDIX A: DERIVATION OF $\Sigma_1(k,\omega)$

Using Eqs. (6) and (31), we find that

$$\frac{\Sigma_1(k,\omega)}{\omega}=\frac{e_{ijm}k_m}{4ik^2}\int\frac{d^3\mathbf{q}}{(2\pi)^3}[B_{ijkl}(-\mathbf{q})-B_{ijkl}(\mathbf{q})]G^0_{kl}(\mathbf{k}+\mathbf{q},\omega). \tag{A1}$$

According to the definitions given in Eqs. (15), (19), and (20),

$$B^{m=2}_{ijkl}(\mathbf{q})=\omega^4\Gamma_2(q)T^2_{ik}(\mathbf{q})T^{-2}_{jl}(\mathbf{q})=\omega^4\Gamma_2(q)m_im_km^*_jm^*_l, \tag{A2}$$

for the mode $m=2$ and

$$B^{m=1}_{ijkl}(\mathbf{q})=\omega^4\Gamma_1(q)T^1_{ik}(\hat{\mathbf{q}})T^{-1}_{jl}(\hat{\mathbf{q}})=\omega^4\Gamma_1(q)(\hat{q}_im_k+m_i\hat{q}_k)\times(\hat{q}_jm^*_l+m^*_j\hat{q}_l), \tag{A3}$$

for the mode $m=1$. Note that for both modes, $B_{ijkl}(-\mathbf{q})=B^*_{ijkl}(\mathbf{q})$, thanks to the convention introduced in Eq. (21). Using the relation $e_{ijl}k_lm_im^*_j=-i\mathbf{k}\cdot\hat{\mathbf{q}}$, the $m=2$ contribution of Eq. (A1) takes the form

$$\frac{\Sigma^{m=2}_1(k,\omega)}{\omega}=\frac{\omega^4}{4k^2}\int\frac{d^3\mathbf{q}}{(2\pi)^3}\Gamma_2(q)\mathbf{k}\cdot\hat{\mathbf{q}}(m^*_km_l+m_km^*_l)G^0_{kl}(\mathbf{k}+\mathbf{q},\omega). \tag{A4}$$

Using Eq. (3) and contracting with respect to tensor indices, this expression reduces to

$$\frac{\Sigma^{m=2}_1(k,\omega)}{\omega}=\int_0^\infty\frac{\omega^2q^2dq}{16k^2\pi^2}\times\int_{-1}^1dc\Gamma_2(q)\frac{kc[-2\omega^2+k^2(1-c^2)]}{\omega^2-k^2-q^2-2kqc+i0^+}. \tag{A5}$$

After symmetrizing the integrand of the integral with respect to c in Eq. (A5), according to $\int dcg(c)=\int dc[g(c)+g(-c)]/2$, Eq. (A5) becomes identical with the $m=2$ contribution of Eq. (35).

The $m=1$ contribution of Eq. (A1) takes the form

$$\frac{\Sigma^{m=1}_1(k,\omega)}{\omega}=\frac{-\omega^4}{4k^2}\int\frac{d^3\mathbf{q}}{(2\pi)^3}\Gamma_1(q)C_{kl}G^0_{kl}(\mathbf{k}+\mathbf{q},\omega), \tag{A6}$$

with $C_{kl}=\mathbf{k}\cdot\mathbf{m}^*\,m_k\hat{q}_l+\mathbf{k}\cdot\mathbf{m}\,\hat{q}_km^*_l-\mathbf{k}\cdot\hat{\mathbf{q}}\,\hat{q}_k\hat{q}_l$. Using the relation $e_{ijl}m_i\hat{q}_jk_l=i\mathbf{k}\cdot\mathbf{m}$, we find $C_{kl}\,\delta_{kl}=-kc, C_{kl}\,k_lk_l=k^3c(1-2c^2), C_{kl}k_k\hat{q}_l=k^2(1-3c^2)/2$, and $C_{kl}\hat{q}_k\hat{q}_l=-kc$. Using these relations in Eq. (A6), we obtain

$$\frac{\Sigma^{m=1}_1(k,\omega)}{\omega}=\int_0^\infty\frac{\omega^2q^2dq}{16k^2\pi^2}\int_{-1}^1dc\Gamma_1(q)\times\frac{-\omega^2kc-k^3c(1-2c^2)+kcq^2-k^2(1-3c^2)q}{\omega^2-k^2-q^2-2kqc+i0^+}, \tag{A7}$$

After symmetrizing again the integrand of the integral with respect to c, Eq. (A7) becomes identical with the $m=1$ contribution of Eq. (36), with the important property that c^2-1 can be factorized in the numerator in Eq. (36).

APPENDIX B: DERIVATION OF EQ. (40)

Using the change of variables $x=q/2\omega$, Eq. (37) can be written as

$$\frac{\Sigma^{m=\pm2}_1(\omega,\omega)}{\omega}=\mp\frac{\omega^4}{8\pi^2}\int_0^\infty xdx\Gamma_{\pm2}(2\omega x)K(x), \tag{B1}$$

where $K(x)$ denotes the integral

$$K(x)=\int_{-1}^1\frac{c^2(1+c^2)dc}{(x-i0^+-c)(x-i0^++c)}, \tag{B2}$$

which can be decomposed in

$$\mathrm{Re}K(x)=-2x^2-\frac{8}{3}+(x+x^3)\ln\frac{|x+1|}{|x-1|}, \tag{B3}$$

and

$$\mathrm{Im}K(x)=\pi x(1+x^2), \tag{B4}$$

if $-1\leqslant x\leqslant1$ and 0 otherwise. The integration over q in Eq. (B1) can be carried out in the complex plane with the function f defined in Eq. (41), which is identical with ReK except for the absence of absolute values and for this reason f is analytical. $\Gamma_2(q)$ has only two poles in the upper half plane $\kappa+i\sqrt{\tau_2}$ and $\kappa-i\sqrt{\tau_2}$, which correspond to x_1 and x_3 in Eq. (40).

Similarly, the imaginary part of $\Sigma^{m=\pm2}_1(\omega,\omega)$ can be obtained from Eqs. (B1) and (B4),

$$\mathrm{Im}\frac{\Sigma^{m=\pm2}_1(\omega,\omega)}{\omega}=\mp\frac{\omega^4}{8\pi}\int_0^1xdx\Gamma_{\pm2}(2\omega x)x(1+x^2), \tag{B5}$$

which can also be calculated analytically as a function of τ_2,κ, and ω.

[1] J. Cheng and R.B. Meyer, Phys. Rev. A **9**, 2744 (1974).
[2] S.A. Brazovkiĭ and G. Dmitriev, Zh. Éksp. Teor. Fiz. **69**, 979 (1975) [Sov. Phys. JETP **42**, 497 (1976)].
[3] V.K. Dolganov, S.P. Krylova, and V.M. Filev, Zh. Éksp. Teor. Fiz. **78**, 2343 (1980) [Sov. Phys. JETP **51**, 1177 (1980)].
[4] R.M. Hornreich and S. Shtrikman, Phys. Rev. A **28**, 1791 (1983).
[5] H. Grebel, R.M. Hornreich, and S. Shtrikman, Phys. Rev. A **28**, 1114 (1983).
[6] D. Bensimon, E. Domany, and S. Shtrikman, Phys. Rev. A **28**, 427 (1983).
[7] J. Ennis, J.E. Wyse, and P.J. Collings. Liq. Cryst. **5**, 861 (1989).
[8] P.J. Collings, Mod. Phys. Lett. B **6**, 425 (1992).
[9] Z. Kutnjak, C.W. Garland, J.L. Passmore, and P.J. Collings, Phys. Rev. Lett. **74**, 4859 (1995).
[10] E.P. Koistinen and P.H. Keyes, Phys. Rev. Lett. **74**, 4460 (1995).
[11] Z. Kutnjak, C.W. Garland, C.G. Schatz, P.J. Collings, C.J. Booth, and J.W. Goodby, Phys. Rev. E **53**, 4955 (1996).
[12] T.C. Lubensky and H. Stark, Phys. Rev. E **53**, 714 (1996).
[13] M.A. Anisimov, V.A. Agayan, and P.J. Collings. Phys. Rev. E **57**, 582 (1998).
[14] B. Pansu, E. Grelet, M.H. Li, and H.T. Nguyen, Phys. Rev. E **62**, 658 (2000).
[15] P. Jamée, G. Pitsi, M.H. Li, H.T. Nguyen, G. Sigaud, and J. Thoen, Phys. Rev. E **62**, 3687 (2000).
[16] E.I. Demikhov and V.K. Dolganov, Kristallografiya **34**, 1198 (1989) [Sov. Phys. Crystallogr. **34**, 723 (1989)].
[17] C. Hunte and U. Singh, Phys. Rev. E **64**, 031702 (2001).
[18] P.J. Collings, Phys. Rev. A **30**, 1990 (1984).
[19] H. Stark and T.C. Lubensky. Phys. Rev. E **55**, 514 (1997).
[20] E.I. Kats, Zh. Éksp. Teor. Fiz. **65**, 2487 (1973) [Sov. Phys. JETP **38**, 1242 (1974)].
[21] P. Galatola, Phys. Rev. E **55**, 4338 (1997).
[22] L. D. Landau and E. M. Lifshitz, *Electrodynamics of Continuous Media* (Pergamon Press, New York, 1960).
[23] T. C. Lubensky and P. Chaikin, *Principles of Condensed Matter Physics* (Cambridge University Press, New York, 1995).
[24] V.K. Filev, Zh. Éksp. Teor. Fiz. **37**, 589 (1983) [Sov. Phys. JETP **37**, 703 (1983)].
[25] P.R. Battle, J.D. Miller, and P.J. Collings, Phys. Rev. A **36**, 369 (1987).
[26] C. Hunte, U. Singh, and P. Gibbs. J. Phys. II **6**, 1291 (1996).
[27] P. G. de Gennes and J. Prost, *The Physics of Liquid Crystals* (Oxford Science, Oxford, 1993).
[28] E.I. Kats, Zh. Éksp. Teor. Fiz. **59**, 1854 (1970) [Sov. Phys. JETP **32**, 1004 (1971)].
[29] V.A. Belyakov, E.I. Demikhov, V.E. Dmitrienko, and V.K. Dolganov, Zh. Éksp. Teor. Fiz. **89**, 2035 (1985) [Sov. Phys. JETP **62**, 1173 (1985)].
[30] U. Singh, P.J. Collings, C.J. Booth, and J.W. Goodby. J. Phys. (France) **7**, 1683 (1997).
[31] G. Pelzl and H. Sackmann. Z. Phys. Chem. (Leipzig) **254**, 354 (1973).